



HHS Public Access

Author manuscript

Nat Neurosci. Author manuscript; available in PMC 2010 December 01.

Published in final edited form as:

Nat Neurosci. 2010 June ; 13(6): 739–744. doi:10.1038/nn.2538.

Sublayer-specific microcircuits of corticospinal and corticostriatal neurons in motor cortex

Charles T. Anderson^{1,*}, Patrick L. Sheets^{1,*}, Taro Kiritani¹, and Gordon M. G. Shepherd¹

Department of Physiology, Feinberg School of Medicine, Northwestern University, Chicago, IL 60611, USA.

Abstract

The mammalian motor system is organized around distinct sub-cortical subsystems, suggesting that intracortical circuits immediately upstream of spinal cord and basal ganglia might be functionally differentiated, too. Here, we show that the main excitatory pathway within mouse motor cortex, layer 2/3→5, is fractionated into distinct pathways targeting corticospinal and corticostriatal neurons, key cell classes involved in motor control. However, connections were selective for neurons in certain sub-layers: corticospinal neurons in upper layer 5B, and corticostriatal neurons in lower 5A. A simple structural combinatorial principle accounts for this highly specific functional circuit architecture: potential connectivity is established by neuronal sub-layer positioning, and actual connectivity within this framework is determined by long-range axonal projection targets. Thus, intracortical circuits of these pyramidal neurons are specified not only by their long-range axonal targets, or their layer or sub-layer positions, but by both, in specific combinations.

Layer-specific patterns of local circuit connectivity are well established for a number of cortical areas 1, 2, including motor cortex 3, 4. However, projection-class specific connectivity patterns have also been described 5–7, presenting an apparent contradiction: how can *both* a neuron's "layer identity" and "projection-class identity" specify its local circuit organization? Which determinant is primary? Further complexity arises from the variety of firing properties, which may be related to projection target 6, 8, 9, but whose relationship to local circuits in neocortex is largely unknown (but see 6). The combinatorial possibilities for these different aspects of pyramidal neuron "identity" are large, and raise fundamental questions of how many distinct neuronal classes there are in neocortex 10, 11.

The local excitatory network in mouse motor cortex is dominated by a single pathway, layer 2/3→5 (ref. 3). Layer 5 pyramidal neurons in motor cortex project to various targets. Two

Users may view, print, copy, download and text and data- mine the content in such documents, for the purposes of academic research, subject always to the full Conditions of use:http://www.nature.com/authors/editorial_policies/license.html#terms

Correspondence and requests for materials should be addressed to G.S. (g-shepherd@northwestern.edu).

*Equal contributions

Supplementary Information accompanies the paper on www.nature.com.

Competing Interests statement: the authors declare no competing interests.

Authors' Contributions statement: All authors participated in designing, conducting, and analyzing the experiments. P.S. performed most corticospinal and C.A. most corticostriatal recordings, and T.K. performed FA imaging. G.S., C.A., and P.S. wrote the paper.

projection classes centrally involved in motor control are corticospinal and corticostriatal neurons, as these represent the cortical origins of what are sometimes termed the ‘pyramidal’ and ‘extrapyramidal’ motor systems, respectively. Although there is evidence for layer 2/3→corticospinal pathways 12, 13, and for layer 2/3→corticostriatal pathways in non-motor frontal cortex 5, the organization of excitatory input pathways to these two cell classes in motor cortex has neither been systematically mapped at a sub-layer level of resolution nor directly compared.

We hypothesized that the layer 2/3→5 pathway comprises distinct corticospinal/corticostriatal parallel pathways. To test this, we labeled corticospinal and crossed corticostriatal neurons by injecting fluorescent beads into, respectively, the contralateral spinal cord and dorsolateral striatum, and mapped their local sources of excitatory synaptic input. We found evidence supporting this hypothesis, and formulated a simple structure/function principle accounting for the observed parallel pathway organization.

Results

Corticospinal neurons’ circuits

Corticospinal neurons were retrogradely labeled by injecting fluorescent beads into the cervical spinal cord. In coronal brain slices containing the contralateral motor-frontal cortex, labeled corticospinal neurons were distributed from upper to lower layer 5B (Fig. 1a). In mouse motor cortex, layer 5B is a relatively thick layer and consists of multiple sub-layers 4, 14.

Local sources of excitatory input were mapped using whole cell recording and glutamate uncaging-based laser scanning photostimulation (LSPS; Methods) (Fig. 1b). Synaptic input maps at first appeared heterogeneous across neurons due to highly variable amounts of input from layer 2/3. An example of a layer 2/3 corticospinal neuron receiving substantial layer 2/3 input is shown in Fig. 1b. However, when maps were ordered according to the cortical depth of the soma, a clear pattern emerged (Fig. 1c,d): inputs from layer 2/3 neurons were strongest for upper layer 5B corticospinal neurons, but fell steeply as a function of increasing soma position towards lower layer 5B. In contrast, relatively weak intralaminar perisomatic inputs from layer 5B were a consistent feature, independent of soma position (Fig. 1c,d). From these data we conclude that local circuits of corticospinal neurons follow a sub-layer specific pattern of connectivity. This pattern is in general agreement with that previously observed for unlabeled layer 5B pyramidal neurons in motor cortex 3, which showed strong layer 2/3 inputs targeting the layer 5A/B border, with extension into layer 5B.

Crossed corticostriatal neurons’ circuits

Corticostriatal neurons were retrogradely labeled by injecting fluorescent beads into the dorsolateral striatum. In coronal brain slices containing the contralateral motor-frontal cortex, labeled “crossed” corticostriatal neurons were distributed from upper 5A to lower 5B (Fig. 2a), a range that was slightly higher-shifted but mostly overlapping with that of corticospinal neurons (cf. Fig. 1a). Crossed corticostriatal neurons constitute a relatively homogeneous subset of neurons having properties of intratelencephalic (IT)-type

corticostriatal neurons, distinct from pyramidal-tract (PT)-type corticostriatal neurons 15–17. The reason for focusing on crossed corticostriatal neurons was that contralateral striatal injections label only IT-type corticostriatal neurons, but ipsilateral striatal injections label both IT- and PT-type corticostriatal neurons. (Except where noted, ‘corticostriatal’ hereafter signifies ‘crossed corticostriatal’.)

Local sources of excitatory input to these corticostriatal neurons were mapped using the same methods and parameters as for corticospinal neurons (Fig. 2b). Again, input patterns varied systematically as a function of the sub-layer positions of the corticostriatal neurons, and again layer 2/3 inputs were strongest (2C,D). However, the pattern was very different from that of corticospinal neurons, as only neurons in lower 5A received strong layer 2/3 inputs; those in upper 5A and anywhere in layer 5B did not (Fig. 2d). While the pattern of layer 2/3 inputs to layer 5A corticostriatal neurons agreed with that of unlabeled neurons 3, the lack of layer 2/3 input to layer 5B corticostriatal neurons did not, and was in sharp contrast to the strong layer 2/3 inputs recorded for corticospinal neurons as reported above.

Highly specific connectivity underlies parallel pathways

To determine whether layer 5B corticostriatal neurons were *selectively* not innervated by layer 2/3 axons, we examined the precise sub-layer and projection-class specificity of layer 2/3→5 synaptic outflow and connectivity onto layer 5 neurons. First, we functionally assayed the laminar profile of layer 2/3 outflow by flavoprotein autofluorescence (FA) imaging, which detects primarily post-synaptic activity in cortical circuits 18, 19. Layer 2/3 stimulation (by focal glutamate uncaging) evoked FA responses both at the stimulation site and in the middle of the cortex, at the layer 5A/B border (Fig. 3a).

Next, we structurally assayed layer 2/3→5 pathways by selectively transfecting layer 2/3 neurons with fluorescent proteins via *in utero* electroporation. This revealed a band of labeled axons also in the middle of the cortex, at the layer 5A/B border, similar to what has been described previously in other cortical regions 20–22 (Fig. 3). Targeting of these axons to the layer 5A/B border was observed both when neurons throughout layer 2/3 were transfected (Fig. 3), and when only neurons in upper layer 2/3 (“layer 2”) were transfected (Supplementary Fig. 1). The laminar profiles of these functional and structural assays of layer 2/3 outflow were almost identical, peaking at the layer 5A/B border with clear extension into upper layer 5B, and extensive overlap with the laminar distribution of corticostriatal somata (Fig. 3b,c).

Coexpression of the light-activated cation channel channelrhodopsin-2 (ChR2) in layer 2/3 neurons enabled us to use ChR2-assisted circuit mapping (CRACM) (Methods) 21 to test the functional connectivity made by layer 2/3 axons onto corticostriatal neurons (Fig. 4). In each labeled slice, we recorded pairs of corticostriatal neurons (sequentially), one located just above and the other just below the layer 5A/B border. Layer 2/3 connections were much stronger to corticostriatal neurons in lower 5A than in upper 5B ($P < 0.05$, paired *t*-test) (Fig. 4a–d).

The foregoing experiments examined layer 2/3→5 connectivity locally; i.e., on the ipsilateral side. Layer 2/3 neurons also project axons across the corpus callosum to the

homotypic region of cortex in the contralateral hemisphere 20–22, raising the question of whether these long-range callosal layer 2/3→5 pathways follow the same pattern of sub-layer specificity observed for local inputs. Corticocortical projections across the callosum are not normally preserved in brain slices because the axons are cut. However, ChR2-expressing axons remain photoexcitable even after scission, and therefore the same experiment could be done looking at contralateral layer 2/3 inputs 21. This showed the same discontinuity at the layer 5A/B border: layer 2/3 connections (from callosally projecting axons, originating from layer 2/3 pyramidal neurons in the contralateral hemisphere) were much stronger to neurons in lower 5A than in upper 5B ($P < 0.05$, paired t -test) (Fig. 4e–h).

Lastly, we recorded from corticostriatal/corticospinal neighboring-neuron pairs of upper 5B neurons and mapped their inputs with glutamate uncaging (Fig. 5). This direct within-slice and within-sub-layer comparison showed that, compared to corticospinal neurons, corticostriatal neurons in upper 5B received much less layer 2/3 input ($n = 5$ corticospinal/corticostriatal pairs; corticospinal/corticostriatal ratio = 9.7 at the peak and 5.7 over the entire region of interest, $P < 0.05$, t -test; Fig. 5d). In contrast, the difference in the amount of layer 5/6 input was much smaller (corticospinal/corticostriatal ratio = 1.8, $P > 0.05$, t -test; Fig. 5d). Corroborating this, analysis of the non-paired input map data sets recorded from corticospinal and corticostriatal neurons (i.e., in separate experiments, shown previously in Fig. 1d and Fig. 2d) showed a similar large difference in input from layer 2/3 to neurons in upper layer 5B, as a function of projection target (Fig. 5e).

These data show that layer 2/3 axons send an excitatory projection to the layer 5A/B border (i.e., to both lower layer 5A and upper layer 5B), where they provide strong input to corticostriatal neurons in lower layer 5A and to corticospinal neurons in upper layer 5B. In contrast, corticostriatal neurons in upper layer 5B, despite their favorable location for layer 2/3 input, received only weak input.

Ipsilaterally labeled corticostriatal neurons

As described earlier, crossed corticostriatal neurons were used in the previous experiments because they constitute a relatively homogeneous population of IT-type corticostriatal neurons. In contrast, neurons projecting to the ipsilateral striatum, though predominantly IT-type 6, 8, also include PT-type corticostriatal neurons. One might therefore expect that the maps of ipsilaterally labeled neurons would mostly follow the pattern observed for crossed corticostriatal neurons, with a small subset instead following the pattern observed for corticospinal neurons. To test this, we recorded from labeled ipsilaterally projecting corticostriatal neurons and mapped synaptic inputs with LSPS (Fig. 6). Neurons in layer 5A received strong layer 2/3 inputs (Fig. 6a), and most neurons in layer 5B received few or no layer 2/3 inputs (Fig. 6b), with a few exceptions (Fig. 6c). Thus, on average, ipsilaterally projecting corticostriatal neurons mostly followed the pattern observed for crossed corticostriatal neurons; that is, layer 5A but not layer 5B neurons received strong layer 2/3 inputs.

Laminar connectivity matrices

For graphical visualization and comparison of the local circuit organization of these two cell types, we computed connectivity matrices representing the laminar sources of excitatory input to corticospinal and corticostriatal neurons (Methods) 3 (Fig. 7). To generate these matrices, the maps for each projection class were pooled, ordered by soma position, and projected onto a single plane by averaging along map rows. Average maps (based on binning the postsynaptic neurons; bin size 1/16 of the cortical thickness) are shown in Fig. 7a and the average vectors in Fig. 7b. The collection of vectors is equivalent to a presynaptic-postsynaptic matrix (Fig. 7c). These matrices are essentially the same as the ‘side views’ shown previously (Fig. 1c and Fig. 2c), except that the data have been binned, averaged, and transposed for display.

The connectivity matrix for corticospinal neurons shows a layer 2/3 hotspot that appears larger in extent than that for the corticostriatal neurons (Fig. 7d). To compare the two matrices directly, we color-coded each on a single-color scale, and merged the two images (Fig. 7e). The merged image showed sharp segregation of layer 2/3→corticospinal and layer 2/3→corticostriatal pathways. On a compressed intensity scale, the layer 2/3 hotspots remained mostly separate, while the layer 5/6 inputs appeared to overlap.

Although the layer 2/3 hotspots are well separated along the postsynaptic axis, it is less clear whether they are so along the presynaptic axis. This is an important point, because separation would be consistent with ‘parallel’ pathway organization, while non-separation could be consistent with either ‘parallel’ or ‘divergent’ organization. To explore this, we computed ‘synaptic output maps’ from the three-dimensional map data arrays (Methods) 3 (Fig. 7e) as a way to visualize the extent to which upper and lower layer 2/3 provided output to corticospinal and corticostriatal neurons. (Rows in connectivity matrices rows correspond to input maps, columns to output maps.) Output maps showed that neurons in upper layer 2/3 (“layer 2”) projected both to corticospinal neurons in upper 5B and to corticostriatal neurons in lower 5A, but not to corticostriatal neurons in layer 5B (Fig. 7f, left). Neurons in middle and lower sub-layers of layer 2/3 projected primarily to corticospinal neurons in upper 5B, with additional weaker projections to corticostriatal neurons in lower 5A, and again little or no output to corticostriatal neurons in layer 5B (Fig. 7f, right).

In a separate analysis, we calculated the average input from layer 2/3 for the two groups of layer 2/3 receiving neurons (corticostriatal neurons in lower layer 5A, and corticospinal neurons in upper layer 5B) (Fig. 7g). Consistent with the output maps, this showed that the profiles for the two cell classes overlapped in upper layer 2/3 but not in mid-to-lower layer 2/3, a region projecting primarily to corticospinal neurons. From these analyses we conclude that the layer 2/3 pathways to corticospinal and corticostriatal neurons in layer 5 are at least partly segregated – that is, ‘parallel’ (Fig. 7h) – insofar as mid and lower layer 2/3 projects primarily to corticospinal and not corticostriatal neurons. Our methods do not resolve whether outputs from upper layer 2/3 to the two cell classes are shared (i.e., divergent pathways) or not (i.e., parallel).

Discussion

These experiments, based on a variety of *in vivo* labeling and *in vitro* circuit mapping tools, provide evidence that mouse corticospinal and crossed corticostriatal neurons receive layer 2/3 excitatory input in a manner that depends on both the precise sub-layer location of the postsynaptic neuron and its long-range projection target.

We propose a structural combinatorial principle that accounts for the local circuit organization described here. Functionally diverse pathways arise combinatorially from two structural parameters: neuronal sub-layer position and long-range axonal projection target. Sub-layer position, which establishes the density of overlap of presynaptic axons with postsynaptic dendrites, establishes *potential connectivity* to provide an anatomical framework of possible connections. *Actual connectivity* is then determined, in an axonal projection-target specific manner, by functional ‘tuning’ within the structural framework. In other words, $Q(r) \sim F(p) * S(r)$, where Q is pathway strength, F is functional connectivity (which depends on the number and weights of actual synapses), p is projection target, S is structural connectivity, and r is sub-layer position. In terms of neurogeometry, F depends on synaptic strength (q) and on the ratio of actual (n_a) to potential (n_p) structural synapses (the “filling fraction”), and S is equal to n_p 23, 24.

Although obviously a simplification, this combinatorial principle captures key aspects of circuit organization, reconciles two otherwise disparate views of cortical circuit specification (i.e., layer- versus projection-class specificity), and offers a quantitative framework to build on. For example, projection-class specific differences in dendritic architecture (an important but second-order parameter) could also be incorporated (e.g. 5, 7, 8, 25, 26). Results from previous studies touching on sub-layer and projection-target “identities” of cortical pyramidal neurons 5, 6, 27 suggest that a combinatorial sub-layer/projection-target principle likely holds for cortical circuits in general.

The scheme proposed here does not preclude the involvement of other factors in specifying the circuit organization of pyramidal neurons. For example, gene expression patterns are sure to play a major role (e.g. 28). However, our scheme predicts that such factors will correlate with either sub-layer location, projection target, or both. Indeed, firing patterns, which correlate with projection class 6, 8, also correlate with specific patterns of local excitatory connectivity, as demonstrated for crossed corticostriatal neurons in the medial agranular cortex in rats 6. In cases where multiple projection classes can share the same firing phenotype 6, 8, projection class cannot be inferred from firing patterns alone, but must be established by retrograde labeling or other means. On the other hand, sub-layer position is a parameter that can be readily determined by analysis of video images.

In this study we focused on direct measurements of functional connectivity, not structural connectivity. The approach taken here is thus complementary to anatomy-based approaches in which structural (potential) connectivity is calculated from axon/dendrite overlap (neurogeometry; Peters’ rule) 23, 24, 29–33. Our findings are broadly consistent with previous findings from direct structure/function comparisons, showing that functional synaptic connectivity in some intracortical pathways appears to follow the form and strength

predicted by axon/dendrite overlap, but in some cases is markedly stronger or weaker than expected, implying microscopic-scale specificity 7, 23, 32, 34.

Indeed, functional connectivity in most of the pathways studied here is broadly consistent with Peters' rule. For example, functional connectivity was high for most postsynaptic neurons located in the same sub-layers as layer 2/3 axons (i.e., lower-5A corticostriatal and upper-5B corticospinal neurons), and low for neurons in the sub-layers that were not targeted by layer 2/3 axons (i.e., upper-5A corticostriatal neurons and both lower-5B corticostriatal and corticospinal neurons). In contrast, connectivity was incongruously low for upper-5B corticostriatal neurons, differing by a factor of ~10 compared to neighboring upper-5B corticospinal neurons (Fig. 1 and Fig. 5) and lower-5A corticostriatal neurons (Fig. 2, Fig. 4, Fig. 5). The low connectivity is not explained by a low density of presynaptic axons: layer 2/3 axons clearly projected to upper layer 5B where these neurons were located (Fig. 1, Fig. 3, Fig. 5, Fig. 7; Supplementary Fig. 1). Nor is the low connectivity likely to reflect differences in dendritic arbors, because (i) arbors of corticospinal and corticostriatal neurons differ by less than a factor of ~2 (ref. 35; see also 5, 7, 8, 25, 26); (ii) a subset of corticostriatal neurons (those in lower layer 5A) did receive strong inputs (Fig. 2, Fig. 4, Fig. 5); and, (iii) in contrast to the difference in layer 2/3 inputs, corticostriatal and corticospinal neurons in upper layer 5B did receive a similar amount of input (within a factor of ~2) from deeper layers (Fig. 1, Fig. 2, Fig. 5, Fig. 7). Although the reduction in input to upper-5B corticostriatal neurons was large it was not absolute. Rather, layer 2/3 inputs occurred but were reduced in amplitude, similar to the amplitude of layer 5 inputs in general (Fig. 1, Fig. 2, Fig. 5). Further experiments are required to identify the specific synaptic mechanisms underlying the connectivity patterns reported here. In general, our findings demonstrate the dual importance of sub-layer and projection target as conjoint determinants of pyramidal neuron microcircuits.

The topographic and functional differentiation of the motor cortex microcircuit into distinct pathways targeting corticospinal or corticostriatal neurons has several potential implications for motor cortex physiology. One is that only a subset of neurons in either cell class receives strong excitation from superficial layers. Another is that it will be important to assess the intra-striatal specificity of layer 2/3-recipient corticostriatal neurons.

Upper-2/3→lower-5A→striatal pathways could preferentially target the striatal matrix compartment (matrisomes), the dopamine receptor 1 (D1) related network, or both 17, 36. In contrast, we did not identify a strong local source of excitatory input to layer 5B crossed corticostriatal neurons, which could project to the striatal patch compartment (striosomes), preferentially avoid the D2-related network, or both 17, 36. However, ipsilateral cortical input to these striatal compartments could arise from layer 2/3 via layer 5B PT-type corticostriatal neurons.

Whether intracortical circuits upstream of the spinal cord and striatum are similarly organized in other species remains to be determined. Although the corticospinal (and corticobulbar) system is ubiquitous (and indeed a defining cortical feature) among mammals 37, it has undergone various evolutionary specializations in different species, including direct projections (corticomotoneuronal connections) onto spinal motoneurons in the primate finger motility system 38, 39 and onto bulbar motoneurons in the rodent vibrissal motility

system 40. In rodents, corticospinal neurons project to spinal interneurons, not to lower motor neurons directly 41, 42. In contrast to these specialized monosynaptic pathways from upper to lower motor neurons, this cortical projection to spinal interneurons (the non-corticomotoneuronal corticospinal system) is evolutionarily older and more conserved among mammals 13, 37. In mice, the motor cortex contains a mapped representation of the body 43, 44, and transgenic mice bearing mutations responsible for human forms of upper motor neuron disease also develop motor symptoms including paralysis 45, 46. The identification of corticospinal/corticostriatal-specific pathways here provides a starting point for evaluating their differential roles in motor control and movement disorders 47, and for investigating the microcircuit-level mechanisms underlying motor behaviors 48.

Supplementary Material

Refer to Web version on PubMed Central for supplementary material.

Acknowledgements

We thank L. Petreanu and K. Svoboda (Howard Hughes Medical Institute, Janelia Farm Research Campus, Ashburn, Virginia), for plasmids and comments, and D. Buxton for advice on retrograde labeling methods. Funded by grants from the Whitehall Foundation and the National Institute of Neurological Disorders and Stroke at the National Institutes of Health (NS061963).

References

1. Thomson AM, Bannister AP. Interlaminar connections in the neocortex. *Cereb Cortex*. 2003; 13:5–14. [PubMed: 12466210]
2. Douglas RJ, Martin KA. Neuronal circuits of the neocortex. *Annu Rev Neurosci*. 2004; 27:419–451. [PubMed: 15217339]
3. Weiler N, Wood L, Yu J, Solla SA, Shepherd GMG. Top-down laminar organization of the excitatory network in motor cortex. *Nat Neurosci*. 2008; 11:360–366. [PubMed: 18246064]
4. Shepherd GMG. Intracortical cartography in an agranular area. *Frontiers in Neuroscience*. 2009
5. Morishima M, Kawaguchi Y. Recurrent connection patterns of corticostriatal pyramidal cells in frontal cortex. *J Neurosci*. 2006; 26:4394–4405. [PubMed: 16624959]
6. Otsuka T, Kawaguchi Y. Firing-pattern-dependent specificity of cortical excitatory feed-forward subnetworks. *J Neurosci*. 2008; 28:11186–11195. [PubMed: 18971461]
7. Brown SP, Hestrin S. Intracortical circuits of pyramidal neurons reflect their long-range axonal targets. *Nature*. 2009; 457:1133–1136. [PubMed: 19151698]
8. Hattox AM, Nelson SB. Layer V neurons in mouse cortex projecting to different targets have distinct physiological properties. *J Neurophysiol*. 2007; 98:3330–3340. [PubMed: 17898147]
9. Miller MN, Okaty BW, Nelson SB. Region-specific spike-frequency acceleration in layer 5 pyramidal neurons mediated by Kv1 subunits. *J Neurosci*. 2008; 28:13716–13726. [PubMed: 19091962]
10. Stevens CF. Neuronal diversity: too many cell types for comfort? *Curr Biol*. 1998; 8:R708–R710. [PubMed: 9778523]
11. Nelson S. Cortical microcircuits: diverse or canonical? *Neuron*. 2002; 36:19–27. [PubMed: 12367502]
12. Kaneko T, Cho R, Li Y, Nomura S, Mizuno N. Predominant information transfer from layer III pyramidal neurons to corticospinal neurons. *J Comp Neurol*. 2000; 423:52–65. [PubMed: 10861536]
13. Rathelot JA, Strick PL. Subdivisions of primary motor cortex based on cortico-motoneuronal cells. *Proc Natl Acad Sci U S A*. 2009; 106:918–923. [PubMed: 19139417]

14. Yu J, et al. Local-Circuit Phenotypes of Layer 5 Neurons in Motor-Frontal Cortex of YFP-H Mice. *Front Neural Circuits*. 2008; 2:6. [PubMed: 19129938]
15. Wilson CJ. Morphology and synaptic connections of crossed corticostriatal neurons in the rat. *J Comp Neurol*. 1987; 263:567–580. [PubMed: 2822779]
16. Levesque M, Charara A, Gagnon S, Parent A, Deschenes M. Corticostriatal projections from layer V cells in rat are collaterals of long-range corticofugal axons. *Brain Res*. 1996; 709:311–315. [PubMed: 8833768]
17. Reiner A, Jiao Y, Del Mar N, Laverghetta AV, Lei WL. Differential morphology of pyramidal tract-type and intratelencephalically projecting-type corticostriatal neurons and their intrastriatal terminals in rats. *J Comp Neurol*. 2003; 457:420–440. [PubMed: 12561080]
18. Shibuki K, et al. Dynamic imaging of somatosensory cortical activity in the rat visualized by flavoprotein autofluorescence. *J Physiol*. 2003; 549:919–927. [PubMed: 12730344]
19. Llano DA, Theyel BB, Mallik AK, Sherman SM, Issa NP. Rapid and sensitive mapping of long-range connections in vitro using flavoprotein autofluorescence imaging combined with laser photostimulation. *J Neurophysiol*. 2009; 101:3325–3340. [PubMed: 19321634]
20. Mizuno H, Hirano T, Tagawa Y. Evidence for activity-dependent cortical wiring: formation of interhemispheric connections in neonatal mouse visual cortex requires projection neuron activity. *J Neurosci*. 2007; 27:6760–6770. [PubMed: 17581963]
21. Petreanu L, Huber D, Sobczyk A, Svoboda K. Channelrhodopsin-2-assisted circuit mapping of long-range callosal projections. *Nat Neurosci*. 2007; 10:663–668. [PubMed: 17435752]
22. Wang CL, et al. Activity-dependent development of callosal projections in the somatosensory cortex. *J Neurosci*. 2007; 27:11334–11342. [PubMed: 17942728]
23. Shepherd GMG, Stepanyants A, Bureau I, Chklovskii DB, Svoboda K. Geometric and functional organization of cortical circuits. *Nature Neuroscience*. 2005; 8:782–790. [PubMed: 15880111]
24. Stepanyants A, Chklovskii DB. Neurogeometry and potential synaptic connectivity. *Trends Neurosci*. 2005; 28:387–394. [PubMed: 15935485]
25. Larsen DD, Wickersham IR, Callaway EM. Retrograde tracing with recombinant rabies virus reveals correlations between projection targets and dendritic architecture in layer 5 of mouse barrel cortex. *Front Neural Circuits*. 2007; 1:5. [PubMed: 18946547]
26. Groh A, et al. Cell-Type Specific Properties of Pyramidal Neurons in Neocortex Underlying a Layout that Is Modifiable Depending on the Cortical Area. *Cereb Cortex*. 2010; 20:826–836. [PubMed: 19643810]
27. Zarrinpar A, Callaway EM. Local connections to specific types of layer 6 neurons in the rat visual cortex. *J Neurophysiol*. 2005; 95:1751–1761. [PubMed: 16319201]
28. Molyneaux BJ, Arlotta P, Menezes JR, Macklis JD. Neuronal subtype specification in the cerebral cortex. *Nat Rev Neurosci*. 2007; 8:427–437. [PubMed: 17514196]
29. Lubke J, Roth A, Feldmeyer D, Sakmann B. Morphometric analysis of the columnar innervation domain of neurons connecting layer 4 and layer 2/3 of juvenile rat barrel cortex. *Cereb Cortex*. 2003; 13:1051–1063. [PubMed: 12967922]
30. Binzegger T, Douglas RJ, Martin KA. A quantitative map of the circuit of cat primary visual cortex. *J Neurosci*. 2004; 24:8441–8453. [PubMed: 15456817]
31. Stepanyants A, et al. Local potential connectivity in cat primary visual cortex. *Cereb Cortex*. 2008; 18:13–28. [PubMed: 17420172]
32. Brown SP, Hestrin S. Cell-type identity: a key to unlocking the function of neocortical circuits. *Curr Opin Neurobiol*. 2009; 19:415–421. [PubMed: 19674891]
33. Binzegger T, Douglas RJ, Martin KA. Topology and dynamics of the canonical circuit of cat V1. *Neural Netw*. 2009; 22:1071–1078. [PubMed: 19632814]
34. Chklovskii DB, Mel BW, Svoboda K. Cortical rewiring and information storage. *Nature*. 2004; 431:782–788. [PubMed: 15483599]
35. Gao WJ, Zheng ZH. Target-specific differences in somatodendritic morphology of layer V pyramidal neurons in rat motor cortex. *J Comp Neurol*. 2004; 476:174–185. [PubMed: 15248197]
36. Gerfen CR. The neostriatal mosaic: striatal patch-matrix organization is related to cortical lamination. *Science*. 1989; 246:385–388. [PubMed: 2799392]

37. Striedter, GF. Principles of Brain Evolution. Sunderland, Massachusetts: Sinauer Associates, Inc.; 2005.
38. Phillips, CG.; Porter, R. Corticospinal neurones: their role in movement. London: Academic Press; 1977.
39. Rathelot JA, Strick PL. Muscle representation in the macaque motor cortex: an anatomical perspective. *Proc Natl Acad Sci U S A*. 2006; 103:8257–8262. [PubMed: 16702556]
40. Grinevich V, Brecht M, Osten P. Monosynaptic pathway from rat vibrissa motor cortex to facial motor neurons revealed by lentivirus-based axonal tracing. *J Neurosci*. 2005; 25:8250–8258. [PubMed: 16148232]
41. Alstermark B, Ogawa J. In vivo recordings of bulbospinal excitation in adult mouse forelimb motoneurons. *J Neurophysiol*. 2004; 92:1958–1962. [PubMed: 15084639]
42. Alstermark B, Ogawa J, Isa T. Lack of monosynaptic corticomotoneuronal EPSPs in rats: disynaptic EPSPs mediated via reticulospinal neurons and polysynaptic EPSPs via segmental interneurons. *J Neurophysiol*. 2004; 91:1832–1839. [PubMed: 14602838]
43. Li CX, Waters RS. Organization of the mouse motor cortex studied by retrograde tracing and intracortical microstimulation (ICMS) mapping. *Can J Neurol Sci*. 1991; 18:28–38. [PubMed: 2036613]
44. Ayling OG, Harrison TC, Boyd JD, Goroshkov A, Murphy TH. Automated light-based mapping of motor cortex by photoactivation of channelrhodopsin-2 transgenic mice. *Nat Methods*. 2009; 6:219–224. [PubMed: 19219033]
45. Hazan J. Spastin, a new AAA protein, is altered in the most frequent form of autosomal dominant spastic paraplegia. *Nat Genet*. 1999; 23:296–303. [PubMed: 10610178]
46. Pasinelli P, Brown RH. Molecular biology of amyotrophic lateral sclerosis: insights from genetics. *Nat Rev Neurosci*. 2006; 7:710–723. [PubMed: 16924260]
47. Ballion B, Mallet N, Bezard E, Lanciego JL, Gonon F. Intratelencephalic corticostriatal neurons equally excite striatonigral and striatopallidal neurons and their discharge activity is selectively reduced in experimental parkinsonism. *Eur J Neurosci*. 2008; 27:2313–2321. [PubMed: 18445222]
48. Dombeck DA, Graziano MS, Tank DW. Functional clustering of neurons in motor cortex determined by cellular resolution imaging in awake behaving mice. *J Neurosci*. 2009; 29:13751–13760. [PubMed: 19889987]
49. Cheatwood JL, Corwin JV, Reep RL. Overlap and interdigitation of cortical and thalamic afferents to dorsocentral striatum in the rat. *Brain Res*. 2005; 1036:90–100. [PubMed: 15725405]
50. Wood L, Gray NW, Zhou Z, Greenberg ME, Shepherd GM. Synaptic circuit abnormalities of motor-frontal layer 2/3 pyramidal neurons in an RNA interference model of methyl-CpG-binding protein 2 deficiency. *J Neurosci*. 2009; 29:12440–12448. [PubMed: 19812320]

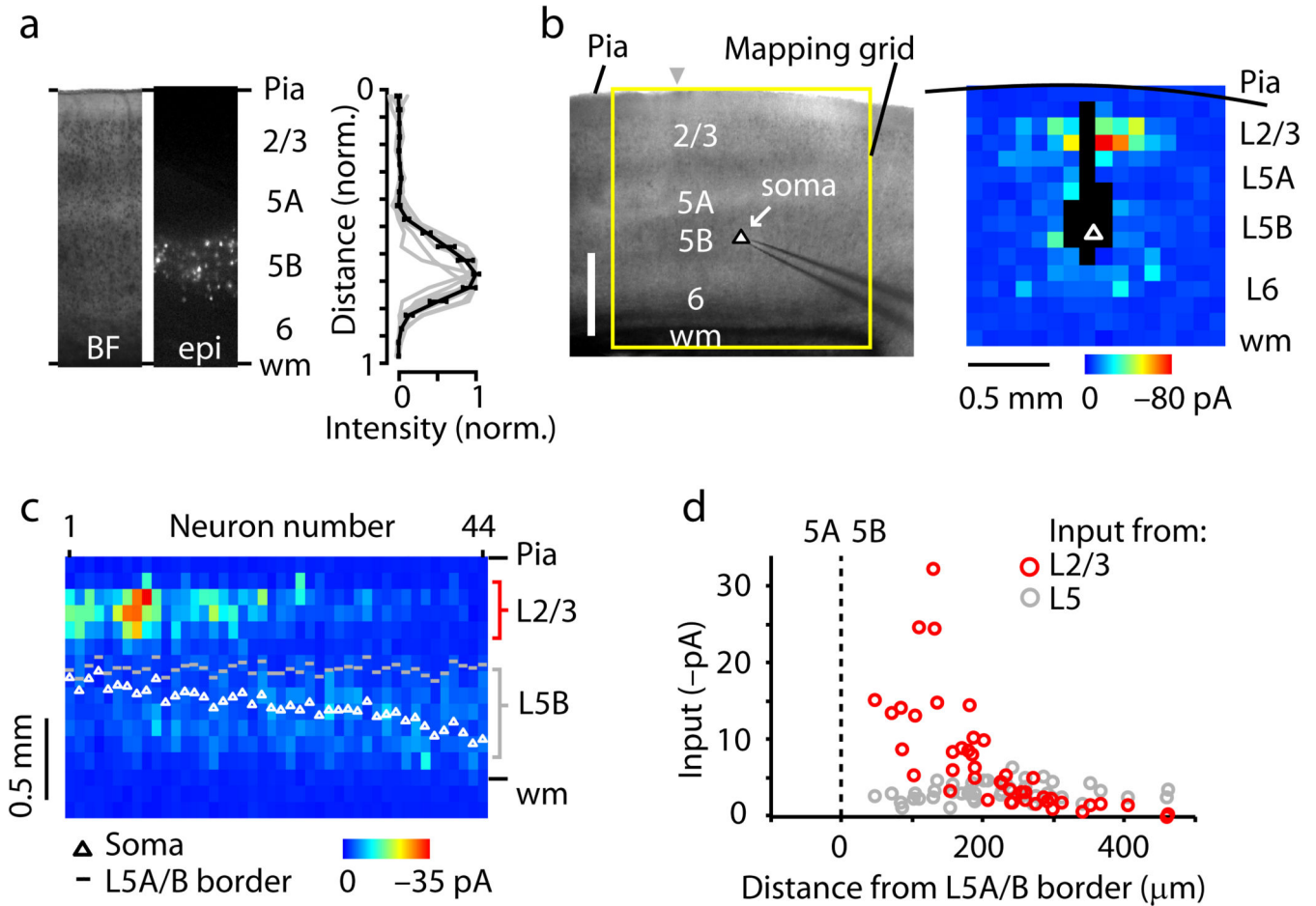


Fig. 1. Sub-layer specific circuits of corticospinal projection neurons. **(a)** Fluorescently labeled corticospinal neurons are distributed across layer 5B in motor cortex. Left, bright-field (BF) and epifluorescence (epi) images; right, normalized fluorescence intensity as a function of normalized cortical distance, where pia = 0 and white matter (wm) = 1. **(b)** Example of a synaptic input map recorded from a corticospinal neuron. **(c)** ‘Side view’ of group of input maps ($n = 44$ corticospinal neurons). Maps were sorted by soma distance from the layer 5A/B border, and the collection of maps was projected onto one plane by averaging along map rows. The absolute distances from the pia to the soma (white circles) and to the layer 5A/B border (gray dashes) are also plotted. **(d)** Layer 2/3 (red) and 5 (gray) input as a function of the distance of the soma from the layer 5A/B border, along the radial axis of the cortex (pia is leftward and white matter is rightward).

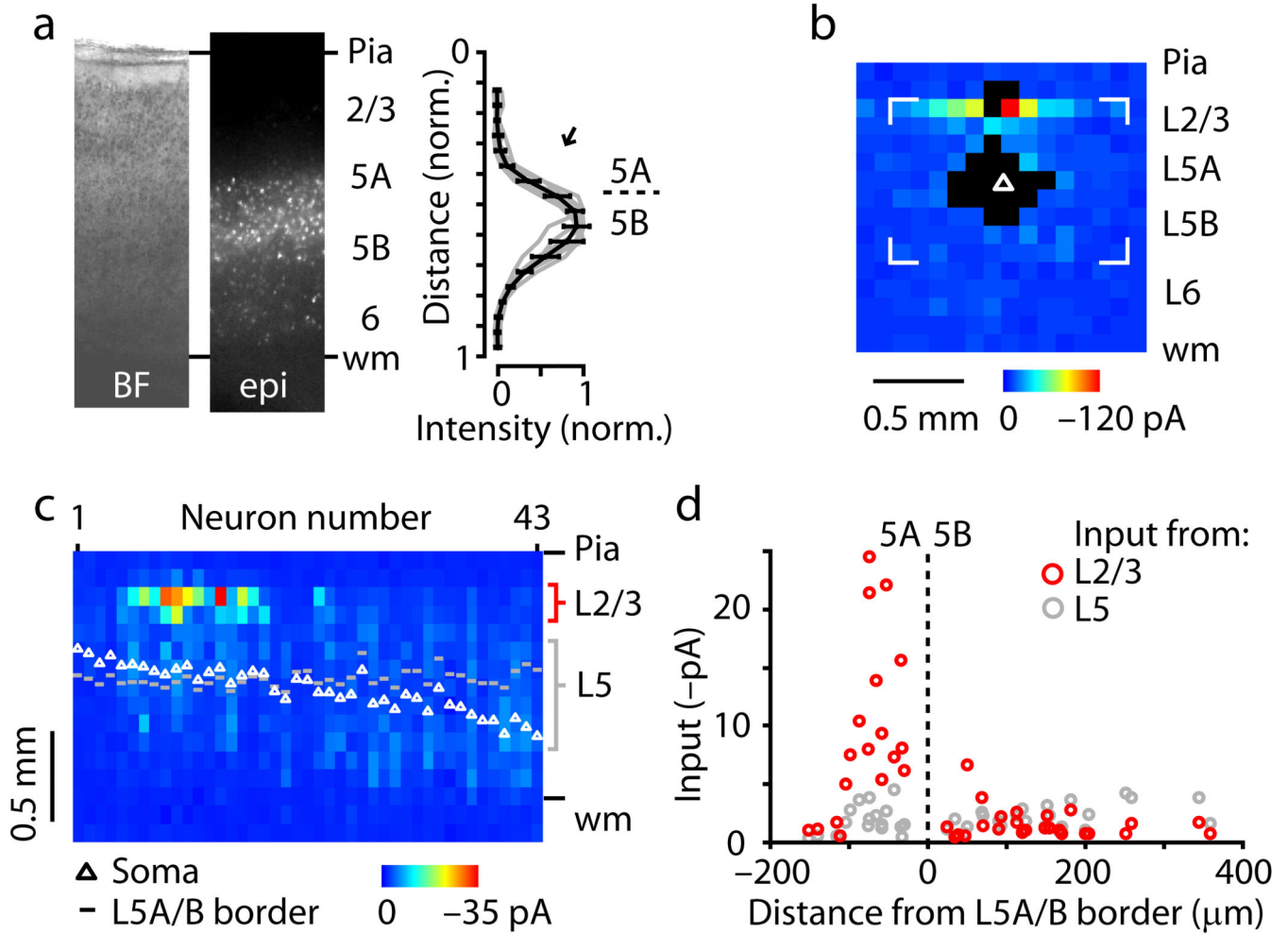


Fig. 2. Sub-layer specific circuits of crossed corticostriatal projection neurons. (a) Laminar distribution of fluorescently labeled neurons. (b) Example of corticostriatal neuron input map. (c) Side view of group of input maps ($n = 43$ corticostriatal neurons). (d) Layer 2/3 (red) and 5 (gray) input as a function of the distance of the soma from the layer 5A/B border, along the radial axis of the cortex (pia is leftward and white matter is rightward).

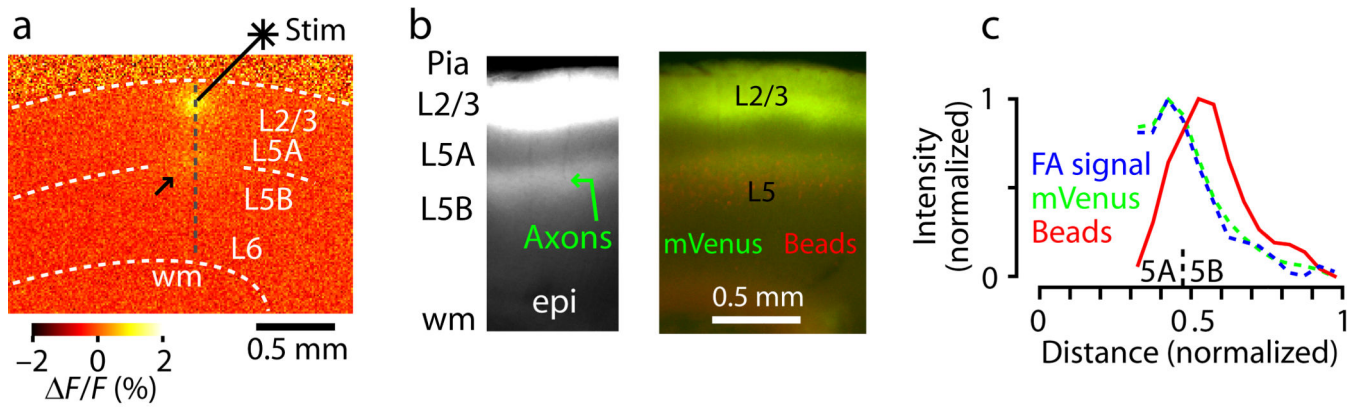
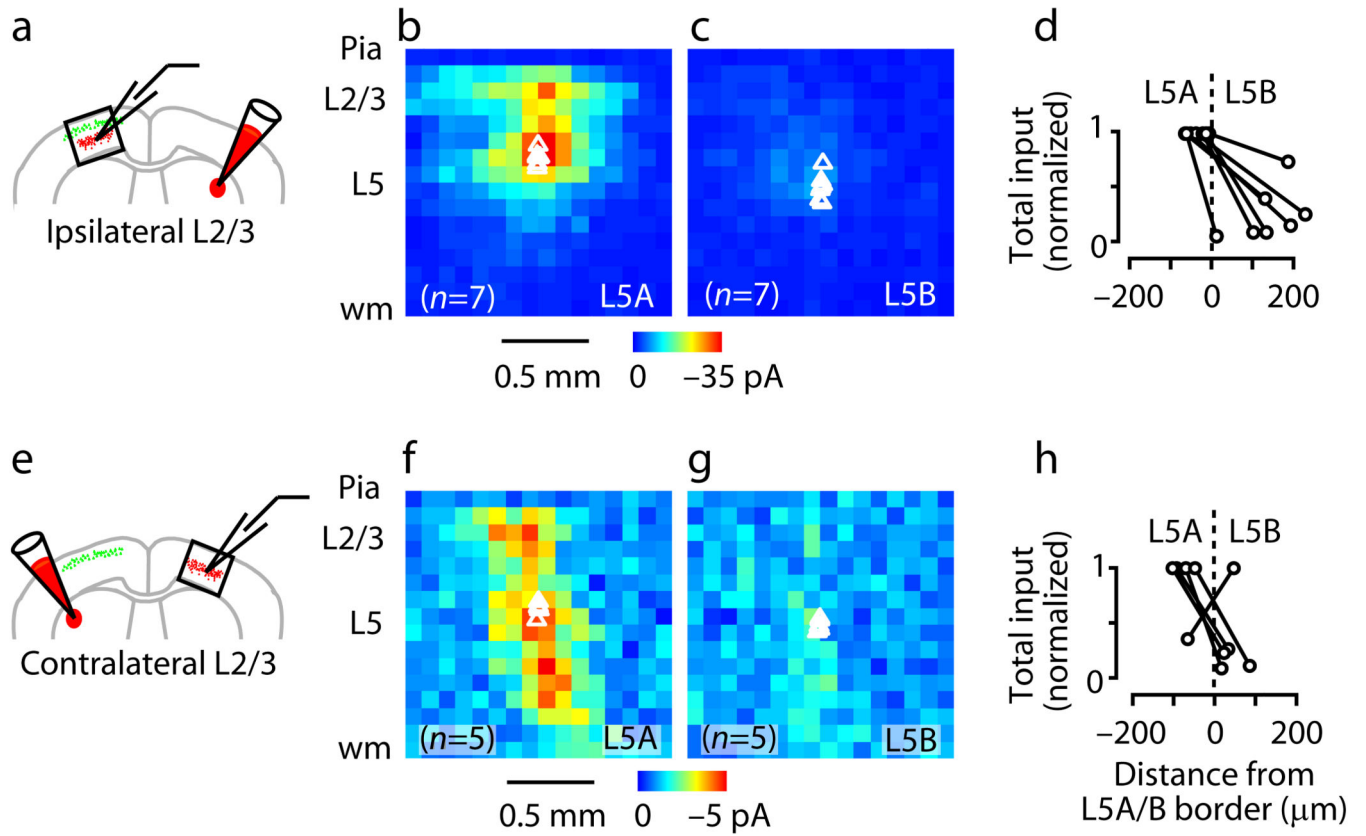


Fig. 3.

Layer 2/3→5 pathways project to the layer 5A/B border. **(a)** Flavoprotein autofluorescence (FA) imaging of activity evoked by focal glutamate photostimulation in layer 2/3. Arrow, hotspot of activity at layer 5A/B border. **(b)** Layer 2/3 neurons expressing fluorescent proteins. Arrow, plexus of fluorescently labeled axons of layer 2/3 neurons, concentrated at layer 5A/B border. **(c)** Comparison of the average laminar profiles of the activity evoked by layer 2/3 stimulation (FA; $n = 6$ slices), the fluorescently labeled layer 2/3 axonal projection to layer 5 (mVenus; $n = 5$ slices), and retrogradely labeled corticostriatal neurons (beads; $n = 7$ slices).

**Fig. 4.**

CRACM analysis of the sub-layer specificity of circuits within the class of crossed corticostriatal neurons, showing that layer 2/3 axons provide input to layer 5A but not layer 5B corticostriatal neurons. (a) CRACM analysis of ipsilateral layer 2/3 projections to corticostriatal neurons. Schematic depicts double-labeling paradigm for examining ipsilateral (local) layer 2/3 inputs to crossed corticostriatal neurons. (b) Average ipsilateral layer 2/3 input to layer 5A corticostriatal neurons. (c) Average ipsilateral input for layer 5B corticostriatal neurons (same color scale). (d) Total ipsilateral input as a function of distance from layer 5A/B border. Recordings were paired (i.e., one layer 5A and one layer 5B neuron) and values normalized to the higher value of the pair. (e) CRACM analysis of contralateral (callosal) layer 2/3 projections to crossed corticostriatal neurons. (f) Average callosal layer 2/3 input to layer 5A corticostriatal neurons. (g) Average contralateral input to layer 5B corticostriatal neurons (same color scale). (h) Total contralateral input as a function of distance from the layer 5A/B border.

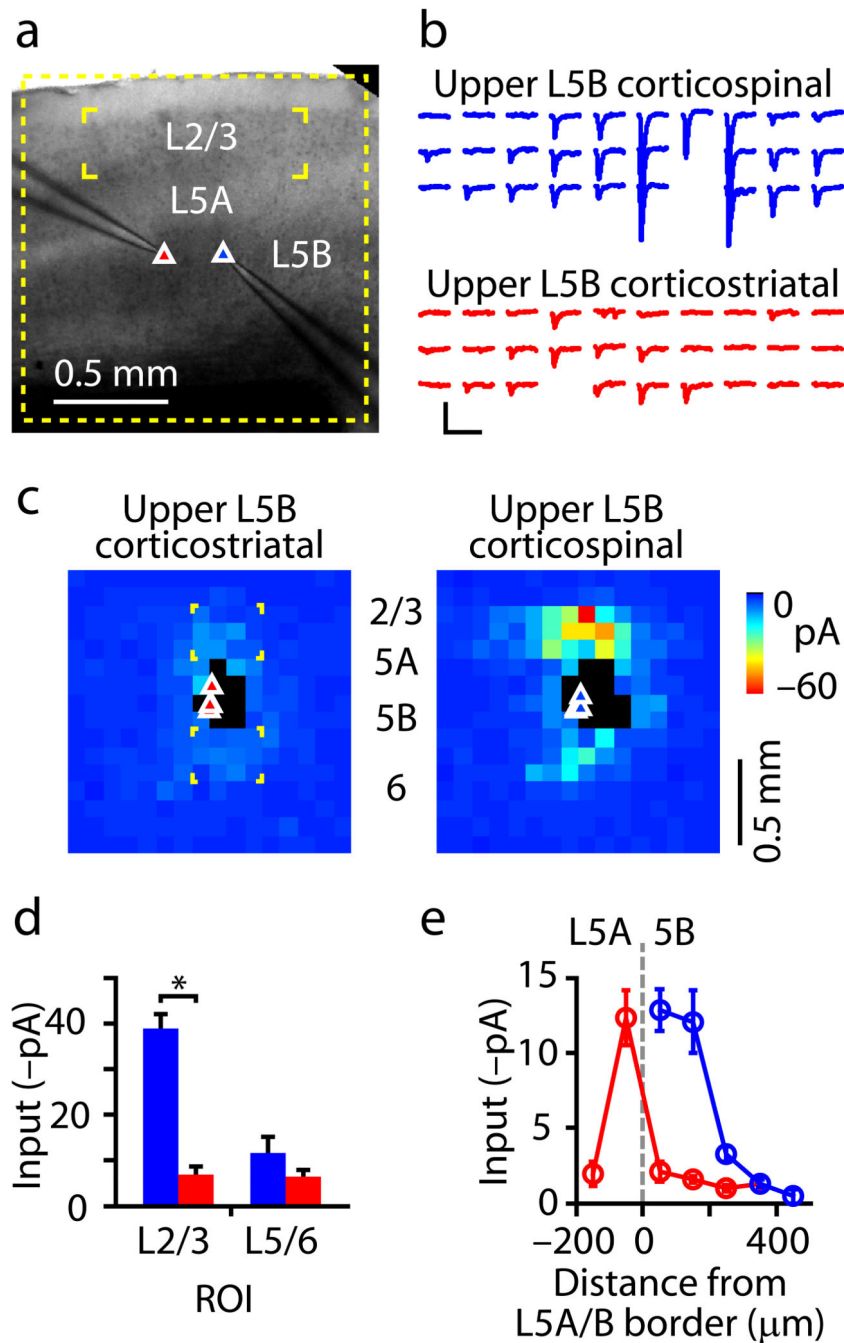


Fig. 5. Pair-mapping analysis of the projection-class specificity of circuits within the same sub-layer, showing that layer 2/3 axons avoid layer 5B corticostriatal neurons, in favor of corticospinal neurons. **(a)** Recording arrangement for simultaneous mapping of layer 2/3 input to a pair of layer 5B corticostriatal (left) and corticospinal (right) neurons. **(b)** Responses across the array of layer 2/3 stimulation sites simultaneously recorded in a corticostriatal (red) and corticospinal (blue) neuron. **(c)** Average maps for (sequentially recorded) corticospinal/corticostriatal pairs, showing lack of layer 2/3 input to corticostriatal

neurons. **(d)** Mean input from layer 2/3 to layer 5B neurons as a function of projection class (blue: corticospinal; red: corticostriatal). ROIs used for this analysis are indicated in panel **c** (bracketed regions on the map on the left). **(e)** Binned (bins: 100 μm) and averaged version of the non-paired corticospinal (blue) and corticostriatal (red) neuron data shown in Fig. 1d and Fig. 2d.

Author Manuscript

Author Manuscript

Author Manuscript

Author Manuscript

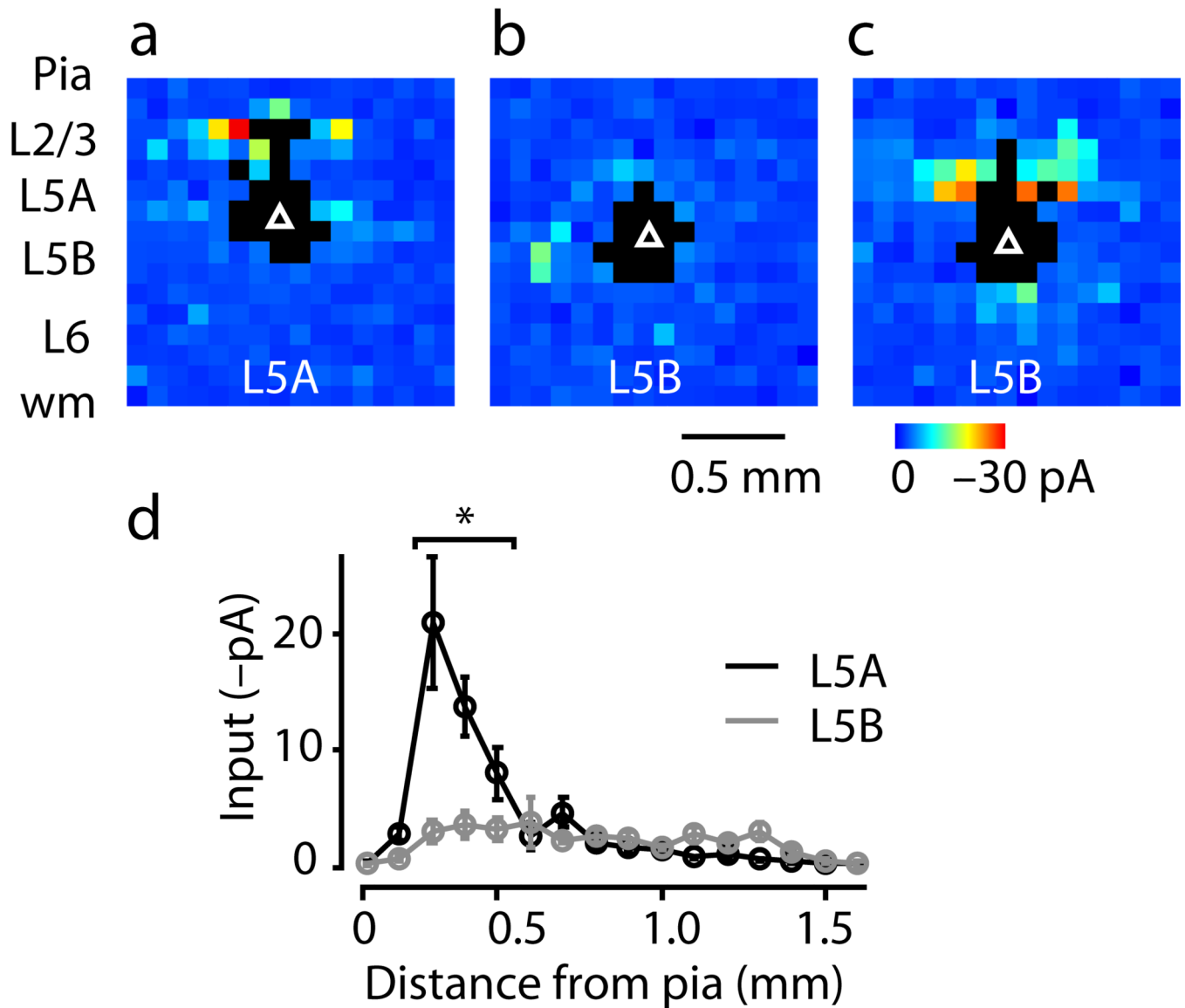
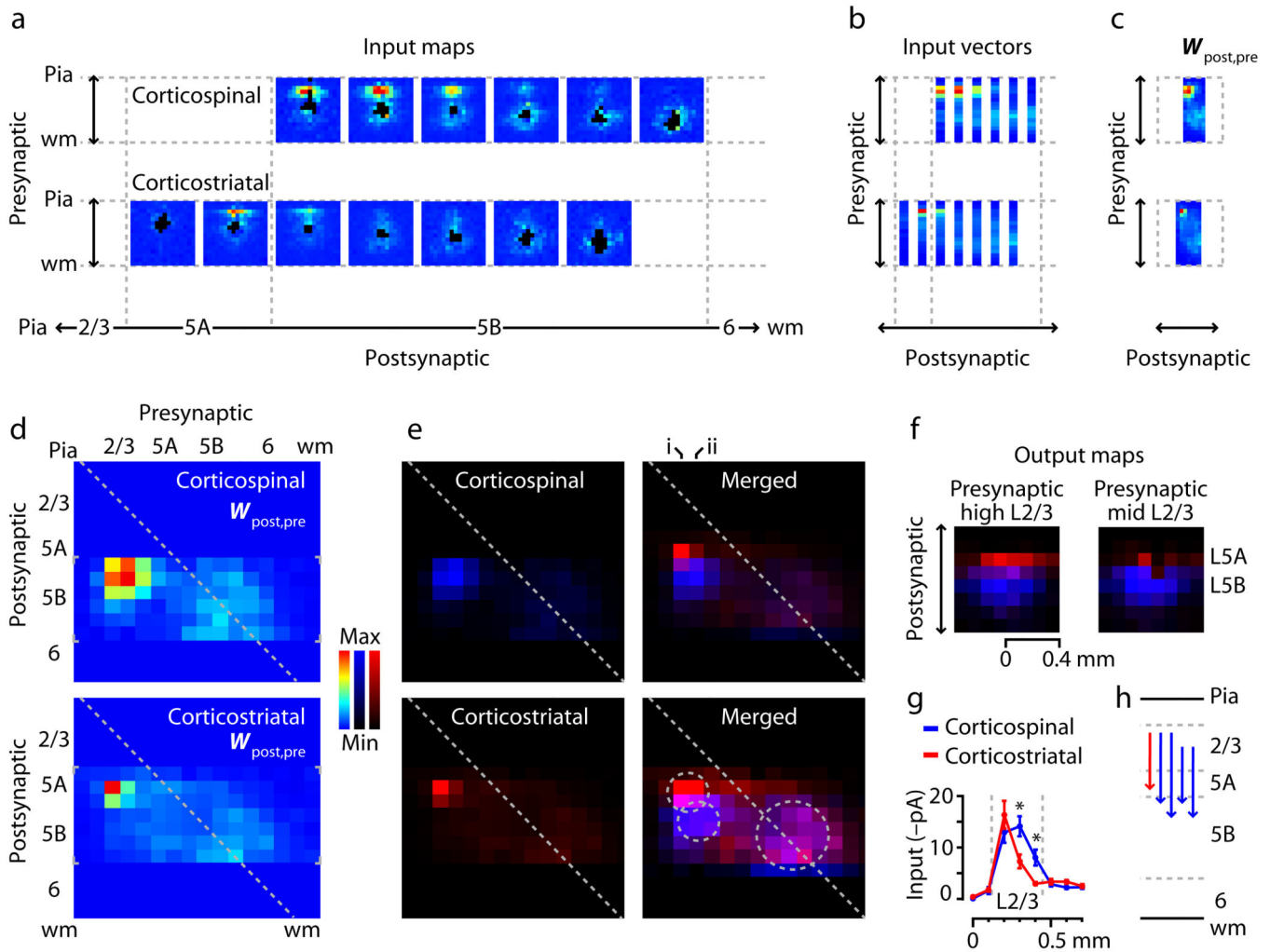


Fig. 6. Input patterns for ipsilaterally projecting corticostriatal neurons, showing that the majority have the same circuit phenotype observed for the crossed corticostriatal neurons. **(a)** Example of a neuron in layer 5A receiving strong layer 2/3 input, mostly from upper layer 2/3. **(b)** Example of a neuron in layer 5B receiving weak layer 2/3 input. **(c)** Example of a neuron in layer 5B receiving strong layer 2/3 input, mostly from lower layer 2/3. **(d)** Synaptic input as a function of presynaptic location (absolute distance of soma from pia). Asterisks indicate map rows where the two cell groups differed significantly ($P < 0.05$, t -test).

**Fig. 7.**

Laminar connectivity matrix analysis, showing partial segregation of L2/3 inputs to corticostriatal and corticospinal neurons. **(a)** Average input maps, generated by sorting individual cells' maps by soma position, binning, and averaging. **(b)** Average input vectors, made by averaging the input maps along map rows. **(c)** The set of input vectors constitutes a laminar connectivity matrix ($W_{post,pre}$). **(d)** Connectivity matrices for the two projection neuron classes. Small gray brackets indicate the data-containing regions. **(e)** Same as in panel **d**, but with the matrices on separate color scales (left; corticospinal: blue, corticostriatal: red) and merged (right; same color scales; magenta represents overlap). Image in lower right is same as in upper right but on a compressed color scale; two smaller circles mark the hotspots of layer 2/3 input, and larger circle marks region of layer 5/6 input. **(f)** Synaptic output maps, computed for presynaptic neurons in upper layer 2/3 (left; corresponds to column *i* in panel **e**) and mid layer 2/3 (right; corresponds to column *ii* in panel **e**). See Methods for details. Color definitions same as for panel **e**. **(g)** Profile of mean input to the two projection neuron classes as a function of presynaptic stimulus location.

Gray lines delimit layer 2/3. Asterisks indicate significant differences ($P < 0.05$, t -test). (**h**)
The strongest quartile of elements in the connectivity matrices, redrawn as arrows.

Author Manuscript

Author Manuscript

Author Manuscript

Author Manuscript